

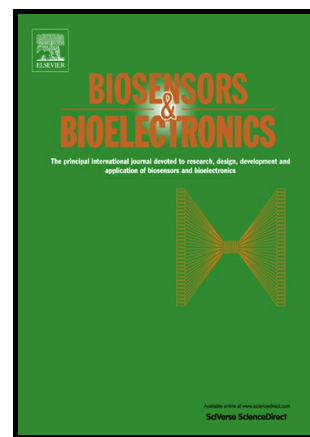
This is the accepted version of the following article:

Peláez E.C., Estevez M.-C., Portela A., Salvador J.-P., Marco M.-P., Lechuga L.M.. Nanoplasmonic biosensor device for the monitoring of acenocoumarol therapeutic drug in plasma. *Biosensors and Bioelectronics*, (2018). 119. : 149 - .
10.1016/j.bios.2018.08.011,

which has been published in final form at
<https://dx.doi.org/10.1016/j.bios.2018.08.011> ©
<https://dx.doi.org/10.1016/j.bios.2018.08.011>. This
manuscript version is made available under the CC-BY-NC-ND
4.0 license
<http://creativecommons.org/licenses/by-nc-nd/4.0/>

Nanoplasmonic biosensor device for the monitoring of Acenocoumarol Therapeutic Drug in Plasma

E. Cristina Peláez, M.-Carmen Estevez, Alejandro Portela, J.-Pablo Salvador, M.-Pilar Marco, Laura M. Lechuga



PII: S0956-5663(18)30599-2
DOI: <https://doi.org/10.1016/j.bios.2018.08.011>
Reference: BIOS10675

To appear in: *Biosensors and Bioelectronics*

Received date: 12 June 2018
Revised date: 30 July 2018
Accepted date: 7 August 2018

Cite this article as: E. Cristina Peláez, M.-Carmen Estevez, Alejandro Portela, J.-Pablo Salvador, M.-Pilar Marco and Laura M. Lechuga, Nanoplasmonic biosensor device for the monitoring of Acenocoumarol Therapeutic Drug in Plasma, *Biosensors and Bioelectronics*, <https://doi.org/10.1016/j.bios.2018.08.011>

This is a PDF file of an unedited manuscript that has been accepted for publication. As a service to our customers we are providing this early version of the manuscript. The manuscript will undergo copyediting, typesetting, and review of the resulting galley proof before it is published in its final citable form. Please note that during the production process errors may be discovered which could affect the content, and all legal disclaimers that apply to the journal pertain.

Nanoplasmonic biosensor device for the monitoring of Acenocoumarol Therapeutic Drug in Plasma

E. Cristina Peláez^{a,b}, M.-Carmen Estevez^{a,b*}, Alejandro Portela^{a,b}, J.-Pablo Salvador^{b,c}, M.-Pilar Marco^{b,c}, Laura M. Lechuga^{a,b}

^aNanobiosensors and Bioanalytical Applications Group (NanoB2A), Catalan Institute of Nanoscience and Nanotechnology (ICN2), CSIC and BIST, Campus UAB Bellaterra, 08193 Barcelona, Spain.

^bNetworking Center on Bioengineering, Biomaterials and Nanomedicine (CIBER-BBN), Spain.

^cNanobiotechnology for Diagnostics group (Nb4D) Department of Chemical and Biomolecular Nanotechnology, Institute for Advanced Chemistry of Catalonia (IQAC) of CSIC, Jordi Girona 18-26 08034 Barcelona, Spain

*Corresponding author. M.-Carmen Estevez: mcarmen.estevez@icn2.cat

Abstract

Acenocoumarol (Sintrom®) is an oral anticoagulant prescribed for the treatment of a variety of thromboembolic disorders such as atrial fibrillation and thrombosis or embolism. It inhibits fibrin production preventing clot formation. Acenocoumarol has a narrow therapeutic range, and its effects depend on several factors, such as body weight, age, metabolism, diet, certain medical conditions or the intake of additional drugs, among others. A higher dose may result in the risk of bleeding, while if it is too low, the risk of blood clot can increase. Complementary tools that allow the therapeutic drug monitoring (TDM) of acenocoumarol plasmatic levels from the starting of the treatment would be of paramount importance to personalize the treatment. Point-of-care (POC) devices can offer an added value in facilitating on-site monitoring (i.e. hospitals, primary care doctor or even by the patient itself) and can aid in dosage management. With this aim, we have developed a compact and simple nanoplasmonic sensing device based on gold nanodisks for the rapid monitoring of acenocoumarol, using highly specific polyclonal antibodies produced against this drug. A specific and reproducible label free indirect competitive assay has been developed and the viability of performing the evaluation directly in plasma diluted 1:1 has been demonstrated. A limit of detection (LOD) of only 0.77 ± 0.69 nM, an IC_{50} of 48.2 ± 5.12 nM and a dynamic range between 3.38 ± 1.33 nM and 1154 ± 437 nM were achieved, which easily fit within the drug plasma levels of acenocoumarol, making this approach a highly attractive option for its decentralized monitoring in human plasma.

Keywords: acenocoumarol; LSPR immunosensor; gold nanodisks; point-of-care device

1. Introduction

The nitrophenyl acetyl-4-oxycoumarin or acenocoumarol (commercialized by Novartis as Sintrom®) is a prescribed oral anticoagulant that belongs to the group of vitamin K antagonists. Acenocoumarol is orally administered as a racemic mixture of R (+) and S (-) optical enantiomers that are rapidly absorbed in the gastrointestinal tract and bind to plasma proteins (>99 %) (Vecchione *et al.*, 2007). It decreases the blood's ability to coagulate, inhibits the formation of fibrin protein that together with platelets forms blood clots. It is employed for the prevention and treatment of a wide variety of thromboembolic disorders such as arterial

fibrillation, deep venous thrombosis and pulmonary embolism (Hadjmohammadi *et al.*, 2012; Lombardi *et al.*, 2003; Schroecksnadel *et al.*, 2013). The sensitivity to these anticoagulants is variable according to each individual and throughout the treatment. Therefore, to ensure the effectiveness and safety of acenocoumarol, the dosage must be accurately adjusted. This implies a narrow therapeutic range and requires regular medical checkups to avoid risks of hemorrhage. The patients under anticoagulants treatment are commonly monitored by determining the International Normalized Ratio (INR), a coagulation parameter resulting from the quotient between the prothrombin time of the patient's plasma and the normal mean prothrombin time (PT) raised to the power of the International Sensitivity Index (ISI) (Locatelli *et al.*, 2005; Hou *et al.*, 2007; Sun *et al.*, 2006). Patients with INR between 2.0 and 4.5 have no recurrence of serious bleeding complications. If the patient's dose is insufficient, the blood will have high coagulation. If the dose is excessive the blood will be excessively anticoagulated and there will be a risk of hemorrhage (Vecchione *et al.*, 2007; Rentsch *et al.*, 2000; Denooz *et al.*, 2009). Currently, there are already several POC coagulometers that measure the clotting time and provide the INR value (i.e. the CoaguChek[®] XS (Roche, Switzerland), i-STAT (Abbott, US) or Coag-Sense[®] (CoaguSense, US), among others). However, these POCs only estimate the quality of INR, but not the quality of oral anticoagulant therapy. Also, the sensitivity of INR is variable in each individual due to the patient's resistance to anticoagulants, the interaction with other medicines and variety of foods mainly rich in vitamin K or other natural products that may interact with the anticoagulant (Osma *et al.*, 2005; Vecchione *et al.*, 2007; Schroecksnadel *et al.*, 2013). Therefore, the direct monitoring of acenocoumarol concentration in plasma could become a complementary tool that can help establish accurate dosing and optimize a truly personalized therapy.

Conventional chromatographic techniques (i.e. GC, HPLC, HPLC-MS) have been employed to evaluate the free fraction of oral anticoagulants in plasma reaching limits of detection (LOD) between 5 and 100 ng mL⁻¹ and a linear range of 15 to 5000 ng mL⁻¹ (Hadjmohammadi *et al.*, 2012; Vecchione *et al.*, 2007; Sun *et al.*, 2006). These methods show good sensitivity and specificity, being able to establish acenocoumarol levels in plasma of 169 - 412 ng mL⁻¹ (479-1167 nM) after 3 hours of administration, and 5 ng mL⁻¹ (14 nM) in approximately 72 hours (Dieterle *et al.*, 1977; Schroecksnadel *et al.*, 2013). But these techniques involve sample pretreatment, expensive extraction procedures and trained personnel, which overall limit the daily monitoring to adapt the medication to the needs of the patients (Locatelli *et al.*, 2005; Huang *et al.*, 2008). Recently, specific antibodies for oral anticoagulants have been produced and an ELISA (Enzyme-Linked Immunosorbent Assay) has been established, achieving LOD good enough to detect the drug directly in plasma (Salvador *et al.*, 2018). However, this method still requires of skilled personnel and laboratory instrumentation to perform the analysis.

Developing a compact, portable POC device, which could be implemented in primary care centers, or even in the household for the patient to monitor itself, would offer significant advantages, as it would facilitate patient's follow up. As there are several factors that can modify the effect of a certain dose of acenocoumarol, a real-time monitoring of the anticoagulant is necessary to assess correct dosage of the drug allowing the patients to improve the self-control of the disease. Optical biosensors are ideal candidates for this application because they can achieve high sensitivity and are easy to operate, offering great benefits in terms of time and sample volume while avoiding sample pretreatment (Tokel *et al.*, 2014; Lopez *et al.*, 2017). We have designed and optimized a portable Localized Surface Plasmon Resonance (LSPR) biosensor device for quantification and monitoring of acenocoumarol in plasma. Nanoplasmonic chips based on gold nanodisks are used as transducer (Soler *et al.*, 2016) and an indirect competitive immunoassay based on the use of specific antibodies has been

implemented. The plasmonic sensor device monitors the variation of refractive index (RI) changes occurring in the nearby of the sensor surface, in this case as a result of the interaction of the antibody over the custom-biofunctionalized antigen-coated surface. This approach allows real-time monitoring of biorecognition events under label-free conditions, avoiding the use of incubation and washing steps and any other additional sample pretreatment. The assay shows excellent detection levels, within the values required in the clinical samples, providing a unique and innovative tool for the monitoring of acenocoumarol in plasma with the potential to be transferred to decentralized settings.

2. Experimental

2.1. Chemicals and immunoreagents

Organic solvents (i.e. acetone, ethanol and dimethyl sulfoxide (DMSO)) and hydrochloric acid 37 % were purchased from Panreac–Applichem (Barcelona, Spain). Alkanethiols (16-mercaptohexadecanoic acid (MHDA) and 11-mercaptoundecanol (MUOH)), 1-ethyl-3-(3-dimethylaminopropyl)carbodiimide hydrochloride (EDC), N-hydroxysulfosuccinimide (NHS)), ethanolamine hydrochloride, Tween 20, dextran sulfate sodium salt (DS, MW ~ 40000 g mol⁻¹), polyvinylpyrrolidone (PVP MW ~ 40000 g mol⁻¹), gelatin from cold water fish skin, chicken serum, bovine serum albumin (BSA), CM-dextran, and all reagents used for the preparation of buffers were acquired from Sigma-Aldrich (Steinheim, Germany). Poly-L-Lysine-graft-PEG (PLL-PEG MW ~ 70000 g mol⁻¹) was purchased from SuSoS (Dübendorf, Switzerland). Diamine-PEG (NH₂-PEG-NH₂, MW 10000 g mol⁻¹) was obtained from Laysan Bio (Arab, AL, USA). Amine-dextran and CHAPS was purchased from Fisher Scientific (Madrid, Spain). Dextran and skim milk powder was purchased from Fluka (Munich, Germany). Pooled normal human plasma was purchased from Innovative Research (USA) and stored at -20 °C until required for further use. The buffers used are the following: PBS 10 mM pH 7.5, PBST-0.05 (PBS with 0.05 % Tween 20), PBST-0.5 (PBS with 0.5 % Tween 20), PBST-DS (PBST-0.5 with DS, 2 mg mL⁻¹), acetate buffer (20 mM pH 5.0), MES buffer (100 mM, 500 mM NaCl, pH 5.5), and HEPES buffer (10 mM pH 7.4).

Acenocoumarol (Sintrom®) was provided by Ipochem Ltd. (Warszawa, Poland). Antigen (hACL-BSA) preparation and production of polyclonal antibody As236 specific for Sintrom have been previously described (Salvador *et al.*, 2018), with the support of the U2 unit (Custom Antibody Service, CAbS) of the ICTS NANBIOSIS.

2.2. Nanoplasmonic chips

Gold nanodisk substrates were fabricated on glass substrates using hole-mask colloidal lithography (HCL) (Fredriksson *et al.*, 2007; Jones *et al.*, 2011). Short-ordered random arrays of gold nanodisks (diameter = 100 nm, height = 20 nm and surface density between 6-7 %) were generated. A schematic representation and a brief description of the fabrication process has been included in Fig S1 in Supplementary Material (SM).

2.3 LSPR biosensor device

A schematic representation of the biosensor can be seen in Fig. 1A. The platform contains all the optical components in a portable 20 x 20 cm² breadboard, which illustrates its potential portability and further integration. The optical components are attached to a triangular platform with a fixed incident angle of the light of 80° on the sensing chip. The nanoplasmonic chips are based on short-ordered arrays of gold nanodisks (Otte *et al.* 2011), whose performance improves the one achieved with regular thin layer gold chips used in conventional Surface Plasmon Resonance (SPR) configuration (Soler *et al.*, 2015). The incident angle (80°) and the

density of disks (6 - 7%) on the surface are key parameters to obtain this improvement in the sensing performance, specially related to the improvement of the surface sensitivity and the signal-to-noise ratio (Otte *et al.*, 2011). The nanoplasmonic chips are clamped between a trapezoidal prism and a flow cell. The sensing area is illuminated with a collimated halogen light (HL-2000, Ocean optics, USA) set in transverse-electric (TE) polarization mode for the LSPR excitation to occur. The reflected light is collected by a fiber-coupled to a CCD spectrometer (Ocean Optics, Jazz Module, US). Reflectivity spectra are acquired (every 3 ms, 300 consecutive spectra) and averaged to provide the spectrum to be analyzed. The obtained spectra show a deep reflectivity at λ_{LSPR} (780 nm) (Fig 1B). The device incorporates a microfluidic system consisting of a flow cell (volume = 4 μL) that is connected to a syringe pump (New Era, NE-1000, USA) which continuously pumps fluid through the sensor surface at a fixed rate. Samples (200 μL) are manually injected by an injection valve (IDEZ Health and Science, V-451, USA). When the samples flow through the sensing area they generate RI changes and therefore a corresponding wavelength displacement in the resonance spectrum (Fig. 1B). These changes are influenced by the difference between the RI of the continuous flow and the sample (bulk effect). On the other hand, chemical interactions occurring at the gold nanodisks surface generate bindings that result in an increment in the mass which translates in an increase in the RI (shifting the resonance curve to higher wavelengths), whereas desorptions decrease the RI on the surface, shifting the curve to lower wavelengths (see Fig. 1). The tracking of the resonance peak (λ_{LSPR}) can be followed in real time via polynomial fit using a homemade readout software, being possible to detect interactions or desorptions as they occur (Fig. 1C).

2.4. Surface functionalization

Nanoplasmonic chips were cleaned by immersing them in acetone, ethanol and Milli-Q water (water Type 1, 18.2 M Ω cm) and then sonicating for 1 min. The chips were dried with a N₂ stream and placed in a UV-O₃ cleaner (BioForce Nanoscience, USA) for 30 min. Finally, they were rinsed with ethanol and dried with N₂ stream. A mixed self-assembled monolayer (SAM) was formed *ex-situ* by incubating the gold nanodisk chips overnight at room temperature with a mixed solution of alkanethiols MHDA:MUOH (ratio 1:5, [alkanethiols] = 250 μM in ethanol). The chips were then thoroughly rinsed with ethanol and dried with N₂ stream. The carboxylic groups were first activated as carbodiimide esters by incubation of a mixed solution of EDC/NHS (0.2 M / 0.05 M) in MES buffer for 30 min and then rinsed with water and dried. Subsequently, the chip was incubated with a solution of the antigen hACL-BSA (50 $\mu\text{g mL}^{-1}$) in 20 mM acetate buffer pH 5.0 overnight at room temperature. The chip was washed to remove unbound hACL-BSA. The remaining unreacted activated carboxylic groups were blocked with an aqueous solution of ethanolamine 1 M pH 8.5 for 5 min. The chips were carefully rinsed with Milli-Q water, dried with N₂ and mounted in the platform. The chip was kept under a continuous flow of PBST-0.5 fixed at 25 $\mu\text{L min}^{-1}$.

2.5. LSPR indirect competitive immunoassay performance

A stock solution of acenocoumarol (10 mM) was prepared in DMSO and used to prepare serial dilutions (from 20 μM to 10 pM) in two different buffers, namely PBST-0.05 and PBST-0.5 (containing 0.05 % and 0.5 % of Tween 20, respectively). A concentration 1/1000 of the specific polyclonal antiserum As236 containing the corresponding antibody was incubated for each analyte concentration during 10 minutes at room temperature. The set of dilutions were injected into the antigen coated surface randomly at a constant rate of 25 $\mu\text{L min}^{-1}$. Free fraction of antibodies not interacting with the analyte are captured by the immobilized antigen conjugate.

A regeneration process allowing the total dissociation of the antigen-antibody interaction, was achieved by injecting a 3 mM NaOH solution for 120 s. Calibration curves were obtained by evaluating different concentrations of analyte three times. The average and standard deviation of $\Delta\lambda_{\text{SPR}}$ was plotted versus logarithmic scale of the analyte concentration. The data was fitted to the following dose-response inhibition equation:

$$y = \frac{D + (A - D)}{1 + \left(\frac{x}{C}\right)^B}$$

where x is the concentration, y is the response signal, A is the asymptotic maximum corresponding to the signal in absence of analyte, B is the slope at the inflection point, C is the inflection point equivalent to the half inhibitory concentration (IC_{50}), and D is the asymptotic minimum corresponding to the background signal. LOD is calculated as the analyte concentration corresponding to 90 % of the signal (IC_{90}). The Limit of Quantification (LoQ) matches the higher limit of the dynamic range of the curve (IC_{80}), set as the interval between the 80 – 20 % of the signal ($IC_{80} - IC_{20}$). The IC_{50} value is commonly used in competitive assays as a value of the sensitivity of the assay (Fig. S3 in SM).

For the evaluation of the plasma effect, experiments were conducted by diluting acenocoumarol in plasma at the same concentrations range described previously. PBST-DS buffer was used as a dilution buffer (1:1) for incubation with the specific polyclonal antiserum As236 and subsequently injected into the sensor. Likewise, in order to evaluate the accuracy of the assay, six blind samples (M1-M6) were prepared in plasma using analyte concentrations within and over, the working range previously obtained. Besides the constant dilution factor of 1:1 in PBST-DS applied to all samples, the blind samples (M3, M6) with concentrations over the working range, required an additional dilution (5 and 10-fold, respectively) to set them in the working range of the sensor. Each measurement using blind samples was repeated at least three times.

3. Results and discussion

3.1. Assay development

The choice of the best immunoassay strategy depends on many factors, being the molecular weight of the analyte the most important one in the case of LSPR sensing, as it is strongly related to the changes of mass on the sensor surface. Small analytes ($MW < 5kDa$) like acenocoumarol ($MW = 353 Da$) induce low RI changes caused by mass changes, therefore, the sensitivity can be limited for a direct detection (Estevez *et al.*, 2012). For this reason, an indirect competitive immunoassay was selected (see Fig. 2). A combination of polyclonal antibodies specifically produced against acenocoumarol (As236) and a related antigen (hACL-BSA) was selected for the assay, due to its superior performance as demonstrated in previously optimized competitive ELISAs (Salvador *et al.*, 2018). Briefly, the antigen is immobilized on the surface of the nanoplasmonic chip and competes for the antibody binding with the free analyte of the sample (acenocoumarol). In this way, the signal obtained is inversely proportional to the concentration of the analyte. This format offers advantages in terms of stability and robustness, as antigens are usually less prone to degradation compared to antibodies and the sensor surface may tolerate better the interaction with plasma samples.

Several parameters affecting the assay performance related to the biofunctionalization of the surface and the detection were evaluated (i.e. SAM composition to attach the antigen, buffer

conditions for the immobilization, assay buffer and immunoreagents concentrations). Gold nanodisks were functionalized following the well-known thiol-modified chemistry, by preparing a mixed SAM with MHDA and MUOH alkanethiols. The carboxylic end provided by MHDA ensures the covalent coupling of the antigen through the BSA carrier, whereas the non-reactive alcohol groups (from MUOH) act as lateral spacers. Different ratios of both compounds were tested (see Fig S4A in the SM), and the amount of antigen immobilized was monitored *in-situ* by the plasmonic sensor, which allows the monitoring of all the steps (see Fig S2 in the SM for a representative example). The results (summarized in Fig. S4A in the SM) show that a higher number of carboxylic groups does not always translate into a higher yield in the covalent coupling. Instead, using a ratio MHDA:MUOH 1:5 (250 μM) resulted in the most efficient coupling, probably due to a better accessibility to the reactive groups ($-\text{COOH}$) on the surface compared with more densely packed SAMs. This ratio of the SAM was selected for further experiments. Additionally, the effect of the pH in the coupling of hACL-BSA was also tested, as it can have a strong influence when the immobilization is done under flow conditions (i.e. the attraction of the antigen over the SAM-modified surface by electrostatic interactions can in turn help enhance the coupling yield). Thus, coupling buffers at different pHs were tested (pH = 4.0, 5.0, 5.5, and 7.4) and the optimal one was found to be acetate buffer 20 mM at pH 5.0 (see Fig. S4B in the SM). Finally, three concentrations of hACL-BSA antigen (10, 20 and 50 $\mu\text{g mL}^{-1}$) were studied (see Fig. S4C in the SM), showing an increasing amount of antigen immobilized as the concentration used was higher. According to our previous experience, $\Delta\lambda_{\text{LSPR}}$ in the order of 4 nm (obtained for $[\text{hACL-BSA}] = 50 \mu\text{g mL}^{-1}$) for the immobilization of BSA-conjugated antigens is usually an optimal value and was therefore initially selected for the assay optimization. The protocol selected *in-situ* was translated to the *ex-situ* approach, by performing successive incubation/washing steps to assess if longer incubation times could have an influence on the overall immobilization. As observed in the Fig. S4D in the SM, similar detection signal was obtained in both cases, indicating that both protocols were equally effective. Therefore, having in mind the final envisaged goal of producing a POC device (i.e., with single-use disposable biofunctionalized chips) we selected *ex-situ* immobilization for the next studies.

Following the immobilization protocol, a non-competitive indirect assay was performed to select the optimal antibody dilution. This is an important factor in competitive immunoassays as it can determine the sensitivity and working ranges of the biosensor. It should provide a signal high enough to allow a wide range of detections under non-saturation conditions. According to this, an As236 dilution of 1/1000 was selected for the competitive assay (see Fig. S5A in SM) as it clearly falls below the saturation of the curve, and provides a $\Delta\lambda_{\text{LSPR}} \sim 1$ nm, which is high enough for the sensor device and its signal-to-noise ratio allows the detection of a wide range of analyte concentrations. The effect of a preincubation step between the antibody and the analyte was also evaluated. A high concentration of acenocoumarol (50 μM , which should result in total inhibition of the signal) was then preincubated with As236 (1/1000) for different periods of time (0, 5, 10 and 15 min, respectively) and then directly injected into the sensor. As shown in the Fig. S5B in SM almost total inhibition is achieved with 10 min, being quite similar for 15 min. Therefore, 10 min was considered enough to ensure the formation of the immunocomplex and was fixed as the incubation time for the competitive assays.

Calibration curves were performed for analyte concentrations ranging from 50 μM to 100 pM. Two different buffers were tested (PBST-0.5 and PBST-0.05, containing different concentration of Tween 20) as shown in the Fig. 3 and Table S1 in SM. A slightly better slope was obtained for PBST-0.05 although we could observe a higher variability with this amount of Tween 20 (i.e. higher SD between replicates). Moreover, a better LOD and IC_{50} were obtained for PBST-0.5. Additionally, the noise was also significantly lower with PBST-0.5 (see sensorgrams in Fig.

S6D, E in SM). According to these results, PBST-0.5 was selected to continue the assay optimization. Finally a competitive indirect assay with the nanoplasmonic biosensor has been established, reaching a LOD of 0.54 nM, an IC_{50} of 76 nM and a linear range response between 3.39 and 1641 nM. The features of the assay are in accordance with the ones obtained by ELISA, with a LOD also below 1 nM (Salvador *et al.*, 2018). The assay in PBST-0.5 is stable and robust, being possible to regenerate the biofunctionalized sensor surface for at least 55 cycles with good repeatability (see Fig. S5C in SM).

3.2. Plasma effect on the acenocoumarol immunoassay

To demonstrate the potential of the assay to be eventually transferred to clinical settings, we evaluated the feasibility of measuring plasma samples. The substances present in blood can negatively affect the assay due to non-specific adsorptions, especially in label-free optical biosensors, where the working principle is directly related with the mass changes occurring on the sensor surface. Therefore, these nonspecific adsorptions can lead to high background signals which may induce alterations in the quantification (Marie *et al.*, 2007; Johansson *et al.*, 2004). Moreover, they may also affect or hinder the antibody-antigen interaction, affecting the assay performance (Estevez *et al.*, 2012).

When plasma 100 % was injected onto the functionalized sensor chip (in the absence of antibody) a strong signal ($\Delta\lambda_{LSPR} = 1.648 \pm 0.02$ nm) was observed, related to a high amount of non-specific interactions. According to this, we decided to test two different conditions but with plasma already diluted 50 % (1:1). Two different set of experiments were studied: (i) introduction of an additional blocking step of the surface and (ii) addition of different additives in the buffer (PBST-0.5) used to dilute the plasma 1:1. Different blocking agents commonly used in immunoassays (Polyvinylpyrrolidone (PVP), skimmed milk, gelatin) were tested as well as those known to be efficient for label-free refractometric sensors, which generate a more biocompatible and antifouling layer (i.e. PEGylated compounds or dextran derivatives), (Marie *et al.*, 2007; Krishnan *et al.*, 2008; Homola *et al.*, 2008). The results are summarized in the Table S2 in SM). The effect of incorporating additives to the dilution buffer is summarized in the Table S3 in SM. We observed that for a 1:1 plasma dilution, none of the blocking agent resulted effective to completely remove the non-specific adsorptions, besides the use of gelatin or PLL-PEG (although it affected also the detection of the antibody). However more interesting results were obtained with the incorporation of dextran sulfate in the buffer (at a concentration of 2 mg mL⁻¹). The nonspecific binding is completely removed as compared to standard PBST-0.5 (see Fig. 4A), and it does not affect the interaction of the antibody with the antigen immobilized on the surface (i.e. the same signal is obtained in PBST-DS and diluted plasma, see Fig. 4B). Under these conditions, the regeneration step remains equally effective using the same regeneration solution. Nevertheless, the injection of plasma solutions somehow affected the robustness of the assay and stability of the antigen coated surface, in such a way the assay was stable only for about 14 cycles before affecting the overall signal (see Fig. S7A in SM) Also, the dextran sulfate in the buffer after 16 cycles reduced its effectiveness as a blocking agent (see Fig. S7B in SM), so the signal increased gradually due to less protection for non-specific adsorptions of the plasma components, affecting the assay. It is worthy to mention that this is not a problem for a future POC, as the sensor cartridge will be intended only for single-use with the patient's sample.

With these updated conditions, two complete calibration curves were obtained, one only in PBST-DS and another in plasma diluted in PBST-DS (1:1). The Fig. S8A and S8B in SM show representative sensorgrams for both assays, at different analyte concentrations. As can be seen in Fig. S8B, the sensorgram shows first an important increase of the signal, resulting from the

bulk effect coming from the plasma samples (i.e. RI increases due to the presence of many components of the matrix compared with the running buffer used, PBST-DS), which is stabilized after all the sample has passed through the cell, resulting in the net signal coming from the interaction of the free Ab with the antigen-coated sensor surface.

As shown in Fig. 4C and Table 1 both curves exhibit similar features in terms of sensitivity and working range, which demonstrates the effectiveness of DS as additive to enable plasma samples analysis. In particular, a LOD of 0.77 nM (0.27 ng mL⁻¹), a LOQ of 3.38 nM (1.19 ng mL⁻¹) and an IC₅₀ of 48.2 nM (17 ng mL⁻¹) have been reached. Although compared with the reported direct competitive ELISA (Salvador *et al.*, 2018), we need a dilution 1:1 of plasma and the IC₅₀ is higher, the LOD achieved is similar and the overall features comfortably allow the direct detection in plasma samples (even after 50 % dilution) according to the reported values found in individuals prescribed with acenocoumarol (both after 3 and 72 hours of drug administration).

3.4. Accuracy study with blind samples

To evaluate the accuracy of the assay, six blind samples of known acenocoumarol concentration (M1-M6) were prepared in plasma whose concentrations are within and over the working range. Samples M3 and M6 required additional dilutions (5 and 10-fold, respectively) to be within the working range. The results are summarized in Table 2. Samples were measured three times with an average recovery between 90 and 100 %. These data indicate a very good correlation with the known concentration, confirming the feasibility of the developed label-free biosensor assay to analyze acenocoumarol in plasma samples. The Fig. S9 in SM show representative sensorgrams for each blind sample showing the shift obtained for each one.

Conclusions

We have successfully implemented a new sensitive, robust and stable label-free immunoassay based on a LSPR biosensor for the control of the anticoagulant drug acenocoumarol in plasma samples. Several parameters have been optimized to enhance the overall assay performance, reaching a LOD of only 0.45 ± 0.05 nM (160 pg mL⁻¹) and an IC₅₀ of 47.5 ± 13.3 nM (16.8 ng mL⁻¹) in buffer conditions. Moreover, the evaluation of plasma after applying a simple 1:1 dilution demonstrates that is enough to maintain the same features (a LOD of 0.77 ± 0.69 nM (272.5 pg mL⁻¹) and an IC₅₀ of 48.19 ± 5.12 nM (17.0 ng mL⁻¹)) with excellent reproducibility and accuracy, as demonstrated with the analysis of blind plasma samples. Overall, these results confirm the usefulness of our approach to monitor acenocoumarol in real samples and demonstrate the feasibility of the LSPR biosensor device to perform fast and reliable analysis. This biosensor could be implemented as a POC as a complementary and useful tool for achieving a personalized therapy follow-up of the acenocoumarol dosage as it allows a rapid and direct quantification requiring a low sample volume. It has to be noted that plasma can be easily obtained from blood by using commercially available centrifugation and filtering tools in a short time of only a couple of minutes. It is estimated that only a few microliters of patient's samples will be sufficient for the analysis. Moreover, LSPR biosensing technology can be easily miniaturised in a portable platform by using not very expensive optical components (as a lamp and a minispectrometer). This platform combined with disposable cartridges incorporating the biofunctionalized sensor chip and a highly efficient microfluidics allowing rapid delivery of the patient's plasma to the sensing area will facilitate the implementation of such platform at affordable cost in decentralized settings such as primary healthcare units, or even in the household environment where patients could make their self-control of the medication.

Acknowledgements

The ICN2 is funded by the CERCA programme / Generalitat de Catalunya. The ICN2 is supported by the Severo Ochoa programme of the Spanish Ministry of Economy, Industry and Competitiveness (MINECO, grant no. SEV-2013-0295). The Nb4D group (formerly Applied Molecular Receptors group, AMRg) is a consolidated research group (Grup de Recerca) of the Generalitat de Catalunya and has support from the Departament d'Universitats, Recerca i Societat de la Informació de la Generalitat de Catalunya (2017 SGR 1441). CIBER-BBN is an initiative funded by the Spanish National Plan for Scientific and Technical Research and Innovation 2013-2016, Iniciativa Ingenio 2010, Consolidar Program, CIBER Actions are financed by the Instituto de Salud Carlos III with assistance from the European Regional Development Fund. The ICTS "NANOBIOSIS", and particularly the Custom Antibody Service (CAbS, IQAC-CSIC, CIBER-BBN), is acknowledged for the assistance and support related to the immunoreagents used in this work.

References

- Denooz R., Douamba Z., Charlier C. J. *Chromatogr. B* 877, (2009) 2344-2348.
- Dieterle W., Faigle J.W., Montigel C., Sulc M., Theobald W. *Eur. J. Clin. Pharmacol* 11, (1977) 367-375.
- Estevez M.-C., Belenguer J., Gomez-Montes S., Miralles J., Escuela A.M., Montoya A., Lechuga L.M. *Analyst* 137, (2012) 5659-5665.
- Fredriksson H., Alaverdyan Y., Dmitriev A., Langhammer C., Sutherland D.S., Zäch M., Kasemo B. *Adv. Mater.* 19, (2007) 4297-4302.
- Hadjmohammadi M., Ghambari, H. *J Pharm Biomed Anal.* 61, (2012) 44-49.
- Homola, J. *Chem. Rev.* 108, (2008) 462-493.
- Hou J., Zheng J., Shamsi, S.A. *J. Chromatogr. A* 1159, (2007) 208-216.
- Huang C., Yang J., Du Y., Miao L. *Clin Chim Acta* 393, (2008) 85-89.
- Johansson M.A., Hellenäs K.E. *Analyst* 129, (2004) 438-442.
- Jones M.R., Osberg K.D., MacFarlane R.J., Langille M.R., Mirkin C.A. *Chem. Rev.* 111, (2011) 3736-3827.
- Krishnan S., Winman C.J., Ober C.K. *J. Mater. Chem.* 18, (2008) 3405-3413.
- Locatelli I., Kmetec V., Mrhar A., Grabnar I. *J. Chromatogr. B* 818, (2005) 191-198.
- Lombardi R., Chantarangkul V., Cattaneo M., Tripodi, A. *Thromb Res* 111, (2003) 281-284.
- Lopez G.A., Estevez M.C., Soler M., Lechuga L.M. *Nanophotonics* 6(1), (2017) 123-136.
- Marie R., Dahlin A., Tegenfeldt J., Höök F. *Biointerphases* 2 (2007) 49-55.
- Osman A., Arbring K., Lindahl T. *J. Chromatogr. B* 826, (2005) 75-80.
- Otte M.A., Estevez M.-C., Regatos D., Lechuga L.M., Sepúlveda B. *ACS Nano* 5 (11), (2011) 9179-9186.
- Rentsch K.M., Gutteck-Amsler U., Bühner R., Fattinger K.E., Vonderschmitt D.J. *J. Chromatogr. B* 742, (2000) 131-142.
- Salvador J.-P., Tassies D., Reverter J.C., Marco M.P. *Anal. Chim. Acta* (2018) <https://doi.org/10.1016/j.aca.2018.04.042>.
- Schroecksnadel S., Gostner J., Jenny M., Kurz K., Schennanch H., Weiss G., Fuchs D. *Thromb Res* 131, (2013) 264-269.
- Soler M., Mesa-Antunez P., Estevez M.-C., Ruiz-Sanchez A.J., Otte M.A., Sepúlveda B., Collado D., Mayorga C., Torres M.J., Perez-Inestrosa E., Lechuga L.M. *Biosens. Bioelectron.* 66 (2015) 115-123.

- Soler M., Estevez M.-C., Villar-Vazquez R., Casal J.I., Lechuga L.M. *Anal. Chim. Acta* 930 (2016) 31-38.
- Sun S., Wang M., Su L., Li J., Li H., Gu D. *J. Pharm. Biomed. Anal.* 42, (2006) 218-222.
- Tokel O., Inci F., Demirci U. *Chem. Rev.* 114, (2014) 5728–5752.
- Vecchione G., Casetta B., Tomaiuolo M., Grandone E., Margaglione M.A. *J. Chromatogr. B* 850, (2007) 507-514.

Accepted manuscript

Fig. 1. (A) Schematic representation of the nanoplasmonic biosensor. (B) Graph showing the displacement of the resonance peak (λ_{LSPR}) to RI changes (photon vs. λ (nm)). (C) Real time monitoring of wavelength displacements ($\Delta\lambda$ vs. time (s)).

Fig. 2. Schematic representation of the biofunctionalization strategy and the indirect competitive immunoassay showing the SAM formation; activation of the carboxylic groups with EDC/NHS; covalent immobilization of antigen and competition step with the sample containing the antibody and acenocoumarol, respectively.

Fig. 3. Standard calibration curves of acenocoumarol immunoassay in PBST-0.5 and PBST-0.05. Each point represents the mean \pm SD of duplicates.

Fig. 4. (A) Effect of DS in the PBST-0.5 used to dilute plasma (1:1) to minimize non-specific binding. (B) Comparison of As236 signal (1:1000) in PBST-DS and in plasma 1:1 diluted in PBST-DS. (C) Calibration curve for acenocoumarol in PBST-DS and Plasma-PBST-DS (1:1). Each point represents the mean \pm SD of three replicates.

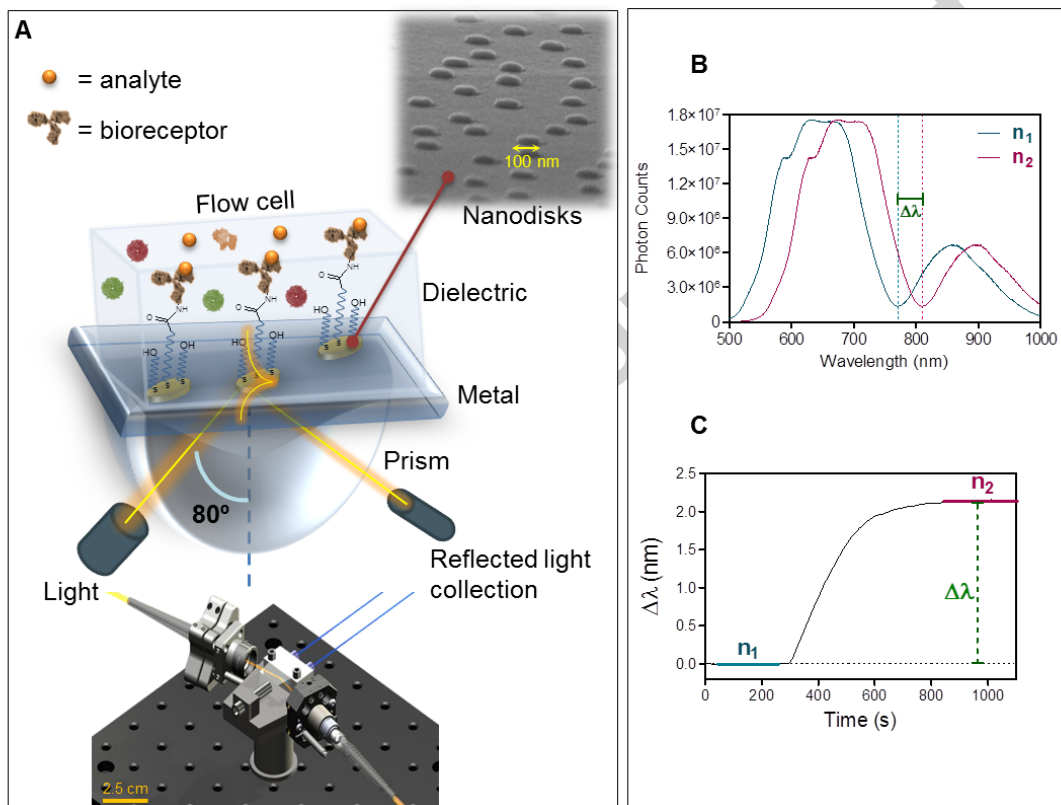


Fig. 1

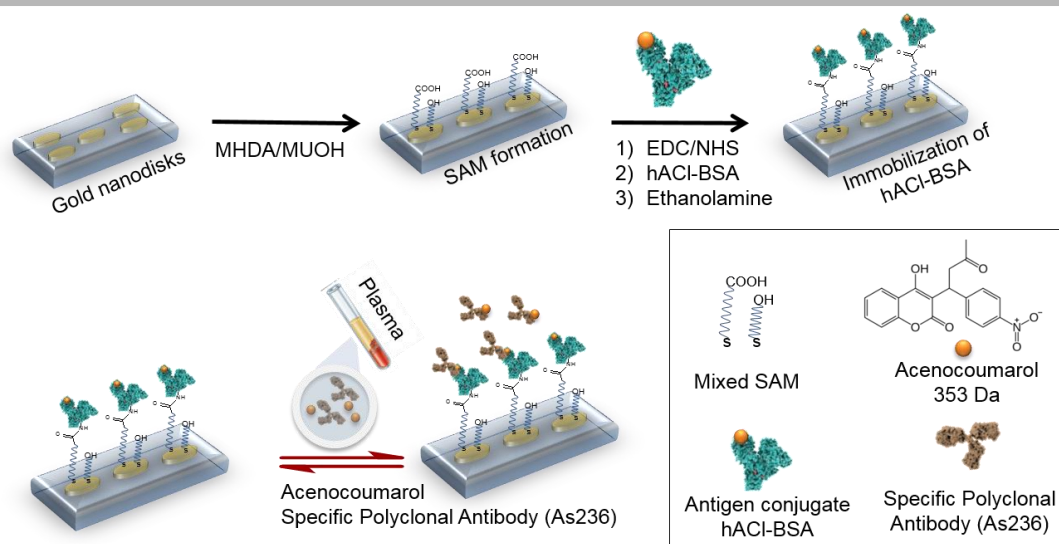


Fig. 2

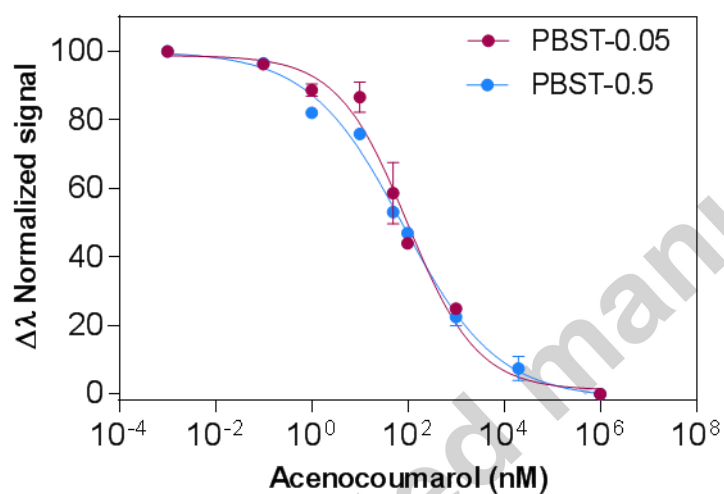


Fig. 3

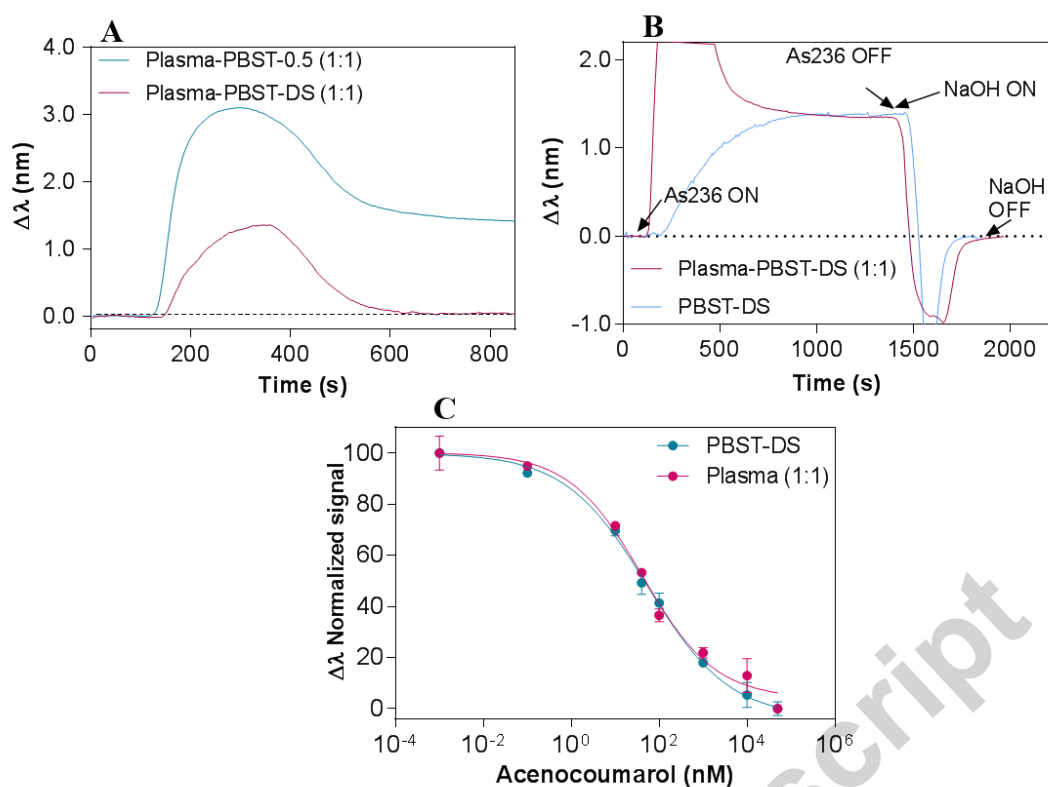


Fig. 4

Table 1. LSPR-based competitive immunoassay features for acenocoumarol detection

	LOD (IC_{90}) (nM)	IC_{50} (nM)	Working range	Slope
	Mean \pm SD	Mean \pm SD	(IC_{80} - IC_{20}) (nM)	
PBST-DS	0.45 ± 0.05	47.5 ± 13.3	$2.54 \pm 0.21 / 761 \pm 264$	-0.47 ± 0.03
Plasma (1:1)	0.77 ± 0.69	48.2 ± 5.12	$3.38 \pm 1.33 / 1154 \pm 437$	-0.52 ± 0.14
ELISA PBST ^{a,c}	0.27 ± 0.09	2.66 ± 0.74	$0.63 \pm 0.20 / 10.19 \pm 6.69$	-0.94 ± 0.06
ELISA Plasma ^{a,b,c}	1.23 ± 0.69	15.73 ± 1.76	$3.09 \pm 1.18 / 80.07 \pm 8.86$	-0.85 ± 0.13

^a: Direct competitive ELISA; ^b: Direct competitive ELISA in undiluted plasma; ^c Data extracted from (Salvador *et al.* 2018).

Table 2. Accuracy study performed with blind samples and the LSPR immunosensor

Samples	Real concentration (nM)	LSPR immunosensor (nM) ^a	Recovery, %
M1	7.0	6.5 ± 1.0	92.3
M2	600	621.1 ± 46.5	103.5
M3	1300	1221 ± 112	93.9
M4	300	301.1 ± 28.8	100.4
M5	25	24.0 ± 1.6	96.2
M6	2000	1810 ± 272	90.5

^a average of three measurements

Highlights

- Implementation of a label-free nanoplasmonic sensing device for the rapid monitoring of acenocoumarol directly in human plasma.
- LSPR biosensor allows the direct quantification of acenocoumarol in real-time while requiring low sample volume.
- Design of a methodology for minimization of non-specific interferences in plasma samples while maintaining the same analytical performance.
- Validation of the accuracy and reliability of the biosensor using blind plasma samples with excellent reproducibility.
- Potential tool that can be implemented as a POC device for monitoring of acenocoumarol in decentralized settings.